International Journal of Heat and Fluid Flow 70 (2018) 271–278

Contents lists available at ScienceDirect

International Journal of Heat and Fluid Flow

journal homepage: www.elsevier.com/locate/ijhff

Drop bouncing by micro-grooves

V. Fink[a], X. Cai[a,b], A. Stroh[a], R. Bernard[1,a], J. Kriegseis[a], B. Frohnapfel[a], H. Marschall[c], M. Wörner[*,d]

[a] Institute of Fluid Mechanics, Karlsruhe Institute of Technology (KIT), Kaiserstr. 10, Karlsruhe 76131, Germany
[b] Institute for Chemical Technology and Polymer Chemistry, Karlsruhe Institute of Technology (KIT), Engesserstr. 20, Karlsruhe 76131, Germany
[c] Mathematical Modeling and Analysis, Technische Universität Darmstadt, Alarich-Weiss Str. 10, 64287 Darmstadt, Germany
[d] Institute of Catalysis Research and Technology, Karlsruhe Institute of Technology (KIT), Engesserstr. 20, Karlsruhe 76131, Germany

ARTICLE INFO

Keywords:
Drop impact
Deposition
Rebound
Structured hydrophobic surface
Phase-field method
Shadowgraphy

ABSTRACT

Micro-textures are a well-known measure to increase surface hydrophobicity. Here, we experimentally investigate the impact of falling water droplets (diameter 2.1 mm, impact speed 0.62 m/s) on flat and structured surfaces made of the same hydrophobic material. While on the flat surface the drop settles with deposition, it bounces from the micro-grooved surface. Numerical simulations with a phase-field method mimicking the experiments do reproduce the different impact outcomes (deposition vs. bouncing) observed on both substrates. The axisymmetric simulation for the flat surface and the three-dimensional simulation for the structured surface employ the same grid size. In addition, the values for capillary width (chosen to be about 1% of the drop diameter) and mobility are the same in both simulations, where in the wetting boundary condition the static contact angle on the flat surface (100.3°) is identically used. Recovering the distinct experimental impingement outcomes in the simulation, though limited to one specific combination of drop diameter and impact speed, highlights the potential of the phase-field method for correctly predicting drop impact phenomena on flat and micro-structured surfaces under adequate resolution. Concerning the instantaneous droplet shape, the agreement between computations and experiments on both substrates is, however, only good till the beginning of the receding phases, whereas thereafter, significant differences are obtained.

1. Introduction

Drop impact on a solid surface is a long-standing research topic since Worthington (1876) performed first studies on this subject in 1876. Nowadays, the process can be recorded with a high-speed camera so that the drop deformation can be observed highly resolved in space and time. Due to its great practical importance in nature and a wide variety of industrial processes, the impact of a drop on a solid surface is intensively studied. The current status with emphasis on experiments is discussed in review papers by Yarin (2006) and Josserand and Thoroddsen (2016).

In recent years, the focus of studies on drop impact has changed from flat to structured surfaces, since modern fabrication techniques allow a precise micro-structuring of surface morphology (Davim and Jackson, 2008) aiming to tune the surface wettability towards hydrophilicity or hydrophobicity (Quéré, 2008; Crawford and Ivanova, 2015). The morphology of the micro-structured surface may have a significant influence on the drop impact behaviour (Khojasteh et al., 2016), similar to that for flat surfaces with different irregular roughness (Range and Feuillebois, 1998). Micro-structuring a surface of a certain material, e.g., by grooves, can influence maximum spreading (Vaikuntanathan and Sivakumar, 2016) and impact outcome (Malla et al., 2017), enhance the intensity of the drop rebound (Kannan and Sivakumar, 2008), and can both suppress and facilitate splashing dependent on surface morphology (Kim et al., 2014). Furthermore, hydrophobic micro-patterning a surface can even cause a drop to rebound, when otherwise deposition occurs (Khojasteh et al., 2016; Malla et al., 2017; Richard and Quéré, 2000; Jung and Bhushan, 2008). Such a behaviour is of interest for several technical applications (e.g., self-cleaning and anti-icing) and is also observed in the present study.

In contrast to experiments, numerical studies on the impact of millimetre-size drops on spatially resolved structured surfaces are rare. Most studies use a two-dimensional approach either with lattice Boltzmann (Moevius et al., 2014; Yagub et al., 2015) and phase-field (Wang et al., 2015) methods or by many-body dissipative particle

* Corresponding author.
E-mail address: martin.woerner@kit.edu (M. Wörner).
[1] present address: University of Stuttgart, Institute of Aerospace Thermodynamics, Pfaffenwaldring 31, 70569 Stuttgart, Germany

https://doi.org/10.1016/j.ijheatfluidflow.2018.02.014
Received 29 September 2017; Received in revised form 8 February 2018; Accepted 26 February 2018

dynamics (Wang and Chen, 2015; Wang et al., 2017). Only recently, full three-dimensional simulations on drop impact on structured surfaces using an advanced geometric volume-of-fluid method (Tan, 2017) and an entropic lattice Boltzmann method (Moqaddam et al., 2017) became available. From these numerical studies, only few consider drop bouncing (Moevius et al., 2014; Wang and Chen, 2015; Wang et al., 2017; Moqaddam et al., 2017).

In the present study, the vertical impact of a 2.1 mm water drop on a flat as well as on a structured horizontal surface made of the same hydrophobic material is investigated. Experiments with a high-speed camera reveal a quite different behaviour of the impacting droplet on the two surfaces. While on the flat surface the impact proceeds in deposition mode, the drop bounces from the substrate structured by micro-grooves before impacting a second time with subsequent deposition. Axisymmetric numerical simulations for the flat surface and full three-dimensional simulations for the structured surface based on the phase-field approach reproduce the distinct experimental impingement outcomes on both substrates, pointing to the potential of the method for predictive computations.

The paper is organized as follows. In Sections 2 and 3, the experimental and numerical methods are introduced. The results on the flat and structured surfaces are presented and discussed in Sections 4 and 5, respectively. Section 6 is devoted to summary and conclusions.

2. Experiment

For the experimental investigation of the impact process, the droplet shape is captured utilizing shadowgraphy technique (Tropea et al., 2007). Fig. 1 illustrates the set-up of the present experiment. A syringe with an inner dispense tip diameter of 0.1 mm is mounted 2 cm above the test surface. The syringe is used to generate single distilled water droplets. Driven by gravity, the droplets fall with a diameter of $D_0 = 2.1$ mm through the quiescent air and reach an impact velocity u_0 of 0.61–0.64 m/s. The drop is illuminated from the back and a high-speed camera “pco.1200 hs” records the shadow image of the impacting droplet with a 120/6 lens at a frame rate of 3200 fps and an exposure time of 15 µs.

The drop impact on two different horizontal test surfaces is investigated. Both surfaces are made of hydrophobic polydimethylsiloxane (PDMS). The first surface is flat while the second one is structured with regular grooves as depicted in Fig. 2. The characteristic dimension of the grooved surface is given by $s = 60$ µm. For the flat PDMS surface, the roughness has been measured. The mean roughness (Ra) is 0.078 µm while the mean roughness depth (Rz) defined as the arithmetic mean value of the single roughness depths of five consecutive sampling lengths is 0.56 µm. The roughness of the ridges of the structured surface has not been measured but is expected to be similar so that the roughness depth would be about 1% of the groove dimension s.

Since the wetting behaviour on the flat surface is assumed to be axisymmetric, the impact process is recorded from one side only. For the structured surface, the impact is investigated consecutively from

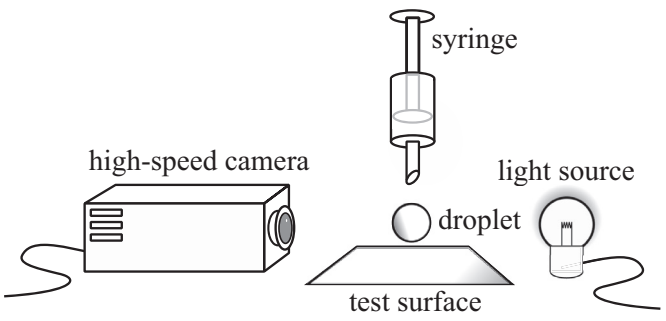

Fig. 1. Schematic of the shadowgraphy set-up.

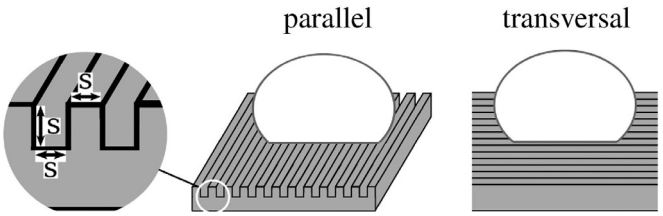

Fig. 2. Geometry of the investigated surface structure (left, $s = 60$ µm) with camera perspectives directed parallel/longitudinal (middle) and transversal (right) to the grooves.

Table 1
Evaluated and averaged initial diameter D_0 and impact velocity u_0 with their standard deviations.

Surface	D_0 [mm]	u_0 [m/s]
Flat	2.086 ± 0.004	0.6072 ± 0.0202
Structured transversal	2.079 ± 0.007	0.6413 ± 0.0348
Structured parallel	2.076 ± 0.005	0.6086 ± 0.0280

two different orthogonal perspectives as illustrated in Fig. 2. In order to minimize the experimental uncertainty, the three experiments are repeated 20 times while the surface is cleaned with isopropyl after each iteration. Table 1 summarizes the average initial (before impact) drop diameter D_0 and impact velocity u_0 for each experiment along with the corresponding standard deviations. The uncertainties in the present work correspond to a 68.2% confidence interval. The impact velocity is determined based on the travelled distance of the droplet from the second last to the last image before impact.

The physical properties of water and air are given in Table 2. The value of the Bond number is $Bo = g\rho_W D_0^2/\sigma \approx 0.59$, where $g = 9.81\text{m}^2/\text{s}$. Accordingly, surface tension forces predominate over gravity and the falling droplets can be considered as spheres which is confirmed by the recorded images. The values of the Reynolds and Weber numbers are $Re = \rho_W D_0 u_0/\mu_W \approx 1300$ and $We = \rho_W D_0 u_0^2/\sigma \approx 11$, respectively.

3. Numerical simulation

3.1. Governing equations

The present simulations are performed by a phase-field method where the gas–liquid interface is considered as a thin transition layer of finite width (Anderson et al., 1998). The spatial distribution of the phases is described by an order parameter C. Here, C takes distinct values $C_W = 1$ and $C_A = -1$ in the liquid and gaseous bulk phases, respectively, and varies rapidly yet smoothly in a thin transition layer. The spatiotemporal evolution of the phase distribution is described by the convective Cahn–Hilliard equation

$$\frac{\partial C}{\partial t} + \nabla\cdot(C\mathbf{u}) = M\nabla^2\phi. \tag{1}$$

In the diffusive term on the right hand side of this equation, M denotes the mobility parameter and ϕ the chemical potential. The latter is defined as

Table 2
Fluid properties.

Parameter	Symbol	Value	Unit
Water density	ρ_W	998.2	kg/m^3
Water viscosity	μ_W	$1.005\cdot10^{-3}$	Pa s
Air density	ρ_A	1.2	kg/m^3
Air viscosity	μ_A	$1.55\cdot10^{-5}$	Pa s
Surface tension	σ	$72.8\cdot10^{-3}$	N/m
Contact angle	θ_{eq}	100.3	°